

Effect of cutting parameters on machining induced distortion in thin wall thin floor parts

Garimella Sridhar, Poosa Ramesh Babu
Mechanical Engineering Department,
University College of Engineering, Osmania University,
Hyderabad, Telangana, India.
Email: garimella_s@yahoo.com

ABSTRACT

This paper presents experimental study on the effect of machining parameters viz., feed, speed, width of cut and depth of cut on machining induced distortion. Machining experiments were done using Response Surface Methodology. Optimization of machining parameters for minimum machining induced distortion was also carried. Four factor, three level Box-Behnken method with analysis of variance is used in dry machining aluminium alloy 2014 T651 with two flute solid carbide \varnothing 10 mm milling tool. Machining simulation experiments were also carried out using Deform 3D software to know the effects of these parameters on forces and temperature generated for correlation with machining induced distortion. Results show that feed, width of cut and depth of cut have significant effect on machining induced distortion. It is observed that, there is an increase in machining induced distortion due to increase in cutting forces in Z – direction and temperature with increase in feed, depth of cut and width of cut during milling thin-wall thin-floor components. The optimal combination of cutting parameters arrived with target values of distortion and twist less than 0.09 mm is feed 0.18 to 0.2 mm/tooth, speed 180 to 210 m/min., width of cut 5.6 mm and depth of cut 0.4 mm.

Keywords: Machining, distortion, thin-wall thin-floor, multi-response, Box-Behnken.

Introduction

Equivalent monolithic thin parts replacing large integrated assemblies by machining them from prismatic blocks removing up to 90 % of material has become quite common in manufacturing shops [1]-[3]. One important

phenomenon during machining these components is distortion, leading to increase in cost of manufacture due to rejections, additional cost for distortion correction and knock on effects due to assembly reworks [3, 4]. Economic losses because of rework and scrap due to distortion was estimated to be \$ 290 million, in a study by Boeing in their four aircraft programs [3, 5, 6]. Distortion during manufacturing of thin-wall, thin-floor parts is due to cumulative effect of several variables in the process like setup configuration, machining parameters, tool geometry, etc., which influence magnitude of machining induced stresses [3,5]. Part distortion is variation from the intended shape after machining and release from the fixture [4]. Distortion is caused by induced stresses due to mechanical and thermal effects during cutting which cause inhomogeneous plastic deformation. Optimization of machining process parameters can significantly control distortion because of control of mechanical and thermal loads which effect final residual stress state of the workpiece [1]. Both, existing bulk and machining induced residual stresses can effect distortion. Magnitude and distribution of residual stresses and part size to thickness ratio dictate distortion. When thickness of workpiece machined is less than 3 mm, machining induced stresses on machined surface will dominate in distorting the part [3, 5, 7, 8].

During the last two decades, many researchers pursued exhaustive study on residual stresses and part distortion during product manufacturing cycle. Hornbach and Prév y [9] conducted simulation and machining experiments on nickel based super alloy disks. They concluded that, when the residual stress distribution is symmetrical then it is possible to predict and minimize distortion. Cui et al., [10] applied Taguchi method to know the effect of deformation caused by heat during cutting of AL 7050/T7451 and found that cutting speed is the most influencing factor which causes deformation due to heat. Dong and Ke [11] carried out comparison of simulation and machining experiments on wing spar made of aluminium alloy AA 7075. Results demonstrated that this method can be used to select optimum machining sequences and tool path. Yeung and Orban [12] developed spiral layer milling tool path which will overcome deflection of thin walls during machining. Jeongjongyun et al., [13] carried out high speed end milling on aluminium alloy 7050-T7451 using Taguchi experimental analysis and concluded that lower the cutting speed, lower the heat deformation and cutting parameters have to be selected as per the shape of the component. Wei and Wang [14] in their study concluded that, when workpiece is longer than its width then the longitudinal residual stresses will have dominating effect on deflection. Younger and Eckelmeyer [15] during manufacturing of aluminium satellite boxes concluded that distortion increases with reduced symmetry. Denken and de Le n [1] have done machining experiments and demonstrated that machining parameters and cutting edge geometry have a definite influence on the residual depth profile and residual stress distribution. Pierard et al., [16] in

their study presented an innovative simulation strategy called level set method, in which shape distortion can be predicted without considering chip formation and tool-workpiece interfacing which can be utilised for optimisation of machining parameters. Guo et al., [17] developed a method of simulation called house-building frame modelling for large scale monolithic multi-frame components which will predict the shape distortion. Bi et al., [18] compared simulation and experiments and predicted distortion with a variation of 19 %. Zhou et al., [19] carried out simulations and found that depth of cut and speed played a minor role and feed rate produced significant effect on residual stress distribution. Tang et al., [20] carried out machining and simulation experiments for predicting machining deformation considering multiple factors along with bulk residual stresses. It was found from the study that process routing has significant effect on machining deformation and double sided symmetric structures distort less during release and redistribution of residual stresses. Yang and Wang [21] conducted machining and simulation experiments and concluded that simulation approach will resolve the distortion problem instead of conducting machining experiments which are time consuming and not economical. Chatelain et al., [22] demonstrated that initial residual stresses in the part has effect on final part distortion. Zhongyi et al., [23] studied residual stress and concluded that the main cause of distortion is distribution of residual stresses in the workpiece. Further, they showed, machining induced residual stresses as main cause for distortion for workpieces machined below 5-6 mm thickness and quenching stresses are responsible for workpieces greater than 10 mm thick. Keleshian et al., [24] performed heat treatment and machining experiments on aluminium alloy 7249 and concluded that water quenching and peak aged components give more warpage. Ye et al., [25] concluded that more fluctuant residual stress distribution was found at the final path of milling on aeronautical monolithic components. Wang et al., [26] studied residual stresses during manufacturing stage. Actual machining distortion was measured after stress-relief using vibration aging method. Guo [27] in his study using theory of elastic mechanics, analysed the mechanism of milling deformation due to residual stresses. Jiang et al., [28] in their study on effect of the tool diameter on residual stresses, concluded that large tool diameter will reduce uncut chip thickness and produce more uniform residual stress distribution. Schulze et al., [29] carried out simulation studies on distortion of T-shaped demonstrator component and concluded that initial residual stresses have significant effect on potential for distortion and increase in cutting forces increase residual stresses. Yang [30] in their study carried out comparison of main effect elements for distortion and concluded that existing bulk residual stress is main element for distortion of aluminium alloy and cutting forces with temperature is the main effect for distortion of titanium alloys. Cao et al., [31] in their machining experiments and FEM on thin walls with different machining

parameters concluded that expensive experiments can be avoided by wall simulation to know the deformation of thin walled machining. Song and Ai [32] in their study on influence of chatter on distortion concluded chatter to be playing vital role in part distortion of thin walled parts. Cerutti and Mocellin [33] used a specially developed finite element tool to predict distortion due to redistribution of existing residual stresses during machining and concluded that fixture layout, forces and cutting sequences can be optimized during design phase itself, before machining. Haiyang et al., [34] used elastic theory model for carrying out simulation experiments on aluminium alloy 7050 on frame shaped workpiece and analysed influence of slots and machining rate on milling deformation. Jain et al., [35] proposed a working methodology for high speed machining using static and dynamic analysis which can be used to mill 0.5 mm thickness wall. Sridhar and Ramesh [36] performed machining experiments on various thickness blanks to know the effect of amount of material removal on distortion and found to have no effect and distortion is significant only below floor thickness of parts less than 3 mm at the same machining conditions. In their experiments on distortion due to milling cutter size they concluded that distortion increases with increase in cutter size at constant feed, speed, depth of cut and material removal rates [37]. Masoudi et al., [38] in their experimental study concluded that Polycrystalline diamond tool is a better alternative to solid carbide tool in reducing distortion in machining thin-walled cylindrical parts.

Although initial residual stresses play major role in distortion of thin-wall thin-floor aluminium components [30], part distortion was also experienced for parts with thickness less than 3 mm [5] even after machining of T651 grade aluminium alloy thin-wall thin-floor components after stress relieving [39] as machining induced distortion is dominant for parts with thicknesses less than 3 mm [5]. So, there is a need for focussed study on direct and interaction effects on machining induced distortion due to four important cutting parameters viz., feed, speed, depth of cut and width of cut which are assignable and controllable by an operator in manufacturing shop. Hence, to understand the effect of these parameters on machining induced distortion and to find optimum parameters for minimum distortion, machining experiments were performed using Response Surface Method (RSM) on thin-wall thin-floor stress relieved demonstrator workpiece made of aluminium alloy 2014 T651.

Experimental procedure

Machining experiments

The workpiece is demonstrative thin-wall thin-floor component shown in Figure 1, made of aluminium alloy 2014 T651 rolled plates which were solution treated, artificially age hardened and stress relieved by stretching.

This is an alloy with copper as major alloying element which has high mechanical strength, fair formability and very good machinability [40]. Blanks used for experiments were cut from rolled plate into blank sizes 110 mm X 45 mm and were milled to the blank size 105 mm X 40 mm. The blanks were then stress relieved. As the blanks used for experiments were taken from same heat number with T651 grade and blanks were stress relieved in a single batch before CNC milling, all the blanks were assumed to be in same physical state with insignificant bulk residual stresses.

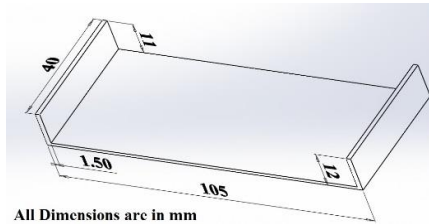
All the machining experiments were carried out using 2 flute, low helix (30°) fine grain solid carbide slot drill Ø 10 mm. New tool is used in each experiment to eliminate the effect of tool wear. Dry machining experiments were carried out on Hardinge Bridgeport 600 P3 3-axis Vertical Machining Centre (VMC) using parallel spiral inside-out tool path. Specially designed vacuum fixture was used for all the components during experiments to hold the part from bottom, to avoid the effect of distortion due to fixture. The vacuum fixture used is shown in Figure 2.

Eighteen equally spaced points were marked on the workpieces before machining on the face opposite to machined face. Distortion is measured on opposite face of machined surface, as measurement of distortion on the machined face will lead to errors due to not perfectly flat or axial drops on the surface. The difference between measurements taken before and after machining operations gives machining induced distortion [8]. Figure 3 shows marked workpiece for measuring distortion. Coordinate Measuring Machine (CMM) was used for distortion measurements. CMM used is Metris LK Integra using CAMIO 4.4 software with specifications: Size 800mm X 700mm X 600mm, Accuracy $1.9 + L/450 \mu$, Repeatability 2.2μ and probe error 3.6μ . During machining, thin-wall thin-floor components not only bow out, but they also get twisted [7, 21]. Twist of the workpiece was measured using feeler gauge. Maximum measurement of distortion and twist used for comparison is shown in Figure 4.

With an aim to study effect of cutting parameters viz., speed, feed, depth of cut and width of cut on machining induced distortion and find optimum parameters for minimization, investigations were done using Box-Behnken Design (BBD), Response Surface Methodology (RSM). RSM is a statistical technique which allows us to investigate relationship between a response and variables influencing the response. BBD is used for non-sequential experiments performed only once. It provides good estimation of first and second-order coefficients, has less design points and are inexpensive to run. All the design points fall within safe operating limits ensuring that all factors are not set at their highest levels simultaneously [41, 42].

In this study, relationship between four factors i.e., cutting speed (V_c), feed (a_f), Depth of cut (a_p), Width of cut (a_e) and output response in terms of distortion (D) and twist (T) were measured. Levels and factors in the

experiments are given in Table 1. The range of factors were selected based on parameters used in a job shop environment. The output in terms of distortion and twist is proposed by nonlinear quadratic equation.



All Dimensions are in mm

Figure 1: Experimental work piece.



Figure 2: Vacuum fixture.

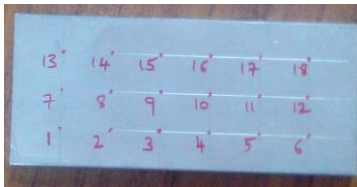


Figure 3: Marking for distortion.

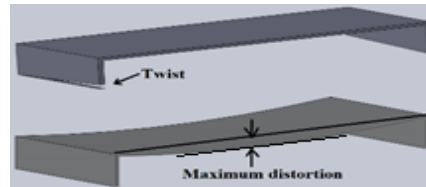


Figure 4: Distortion and twist.

Table 1: Factors and levels in experiment.

Factors	Levels		
	Level 1	Level 2	Level 3
Speed, V_c (m/min.)	100	175	250
Feed, a_f (mm/tooth)	0.05	0.125	0.2
Depth of cut, a_p (mm)	0.4	1.2	2
Width of cut, a_e (mm)	5	6.5	8

Another aim of the experiment is multiple response optimization of both distortion and twist. One such useful approach is technique popularized by Derringer and Suich (1980) using desirability function [41]. The technique translates predicted responses into scale free desirability ranging from 0 to 1. Factor settings with maximum desirability gives optimum parameter condition. The individual desirability function for objective type, minimum response value which is used in this study is given by Equation (1) [41], where d is individual desirability, U is upper limit, y is response and r is exponential parameter that determines the desirability function shape. Equation (2) gives composite desirability which is weighted geometric mean of individual desirabilities, where D_T is complex desirability and n is number of responses for same importance for all responses which are used in the study. Minitab 16

statistical software was used for BBD and response optimization using desirability function.

$$d = \begin{cases} 1 \left(\frac{U-y}{U-T} \right)^r & y < T \\ 0 & T \leq y \leq U \\ 0 & y > U \end{cases} \quad (1)$$

$$D_T = (d_1 * d_2 * \dots * d_n)^{1/n} \quad (2)$$

Simulation experiments

In order to understand the characteristics of machining, vis-à-vis machining parameters (feed, speed, depth of cut and width of cut) and to understand the physics behind distortion and twist, simulation experiments were carried out with 4 factors and 3 levels as per Table 1 and Table 2 similar to machining experiments, using commercial software Deform 3D. The tool and the work piece were modelled in SolidWorks and were imported to Deform 3D as .stl files. Simulations were carried out using incremental Lagrangian formulation with implicit integration method. The solver used is conjugate-gradient with direct integration method. The material properties and flow stress were taken from Deform 3D library [43] with tool material as 10 % cobalt and work piece material as Aluminium alloy 2014. In these simulations the tool was defined rigid and was given thermal properties as it is much harder than workpiece. The work piece is defined as plastic and was given both mechanical and thermal properties. The workpiece fixed from the bottom by defining bottom surface as zero degrees of freedom. The initial temperature of workpiece and tool was defined at 20° C. Tetrahedron mesh was defined for both tool and work piece. Since milling involves high deformations at high strain rates, Deform3D uses adaptive meshing technique where in more elements are used at higher strain rates and lesser elements at lower deformations for accuracy of solution [44]. Small model was used in performing the simulation experiments for computational efficiency. Without compromising on model integrity, a short material length of 1 mm at full width of cut, was chosen to save computational time with simulation steps of 1° per revolution. Average predicted force in X, Y and Z, torque and temperature were calculated with instantaneous simulation data for a cutter stroke of 1 mm.

Results and analysis

Maximum values of distortion and twist for each of the 27 experiments performed were used for analysis to find direct and interaction effects of cutting parameters. Table 2 shows the values of maximum distortion and twist. The average instantaneous cutting force values in X, Y, Z direction, torque and

temperature in the cutting zone resulting from simulation experiments are shown in Table 3.

Table 2: Experimental data using BBD with results.

Std. ord.	Run ord.	Feed (a_f) (mm/tooth)	Speed (V_c) (m/min.)	Depth of cut (a_p) (mm)	Width of cut (a_e) (mm)	Distortion (D) (mm)	Twist (T) (mm)
25	1	0.125	175	1.2	6.5	0.3	0.25
24	2	0.125	250	1.2	8	0.47	0.42
5	3	0.125	175	0.4	5	0.09	0.18
6	4	0.125	175	2	5	0.65	0.73
23	5	0.125	100	1.2	8	0.48	0.46
16	6	0.125	250	2	6.5	0.8	0.75
12	7	0.2	175	1.2	8	0.72	0.65
15	8	0.125	100	2	6.5	0.81	0.84
20	9	0.2	175	2	6.5	1.1	1.05
2	10	0.2	100	1.2	6.5	0.58	0.48
9	11	0.05	175	1.2	5	0.19	0.27
3	12	0.05	250	1.2	6.5	0.25	0.2
18	13	0.2	175	0.4	6.5	0.14	0.1
26	14	0.125	175	1.2	6.5	0.27	0.25
1	15	0.05	100	1.2	6.5	0.19	0.23
7	16	0.125	175	0.4	8	0.18	0.25
8	17	0.125	175	2	8	0.95	0.95
11	18	0.05	175	1.2	8	0.31	0.35
27	19	0.125	175	1.2	6.5	0.28	0.28
21	20	0.125	100	1.2	5	0.26	0.27
14	21	0.125	250	0.4	6.5	0.12	0.15
17	22	0.05	175	0.4	6.5	0.17	0.25
19	23	0.05	175	2	6.5	0.52	0.5
13	24	0.125	100	0.4	6.5	0.13	0.13
10	25	0.2	175	1.2	5	0.42	0.37
4	26	0.2	250	1.2	6.5	0.47	0.36
22	27	0.125	250	1.2	5	0.22	0.3

$$T = 0.26 + 0.1 * a_f - 0.0191 * V_c + 0.3133 * a_p + 0.08 * a_e + 0.0445 * a_f^2 + 0.017 * V_c^2 + 0.1783 * a_p^2 + 0.09 * a_e^2 - 0.0225 * a_f * V_c + 0.175 * a_f * a_p + 0.05 * a_f * a_e - 0.0275 * V_c * a_p - 0.0175 * V_c * a_e + 0.0375 * a_p * a_e \quad (3)$$

$$D = 0.283 + 0.15 * a_f - 0.01 * V_c + 0.333 * a_p + 0.106 * a_e + 0.065 * a_f^2 + 0.03 * V_c^2 + 0.14 * a_p^2 + 0.05 * a_e^2 - 0.0425 * a_f * V_c + 0.1525 * a_f * a_p + 0.045 * a_f * a_e + 0.0075 * V_c * a_e + 0.0525 * a_p * a_e \quad (4)$$

Analysis of experimental results

Experimental results were used to model second order response surface for dependent variables i.e., distortion, and twist using RSM in Minitab 16. Equation (3) and Equation (4) give the predicted model for distortion, D and

twist, T respectively. Test of ANOVA, to justify goodness of fit for the developed empirical relations as shown in Table 4 for distortion, show that the regression Equation (3) is significant as the P-value (0) is less than 0.01 and lack of fit (0.427) is insignificant as it is more than 0.01. R-squared value of the model is 99.78 % indicating that the model can explain 99.78 % of variation [45]. Test of ANOVA as shown in Table 4 for twist show that the regression Equation (4) is significant as P-value (0) is less than 0.01 and lack of fit (0.359) is insignificant as it is more than 0.01. R-squared value of the model is 99.59 % indicating that the model can explain 99.59 % of variation of twist [45].

Table 3: Simulated average values of forces, torque and temperature.

Std. Order	Run Order	Average force (X, Y, Z)			Torque (N mm)	Temperature (°C)
		Fx (N)	Fy (N)	Fz (N)		
1	1	38.39	21.05	26.67	198.06	120.30
24	2	41.06	20.57	30.44	218.04	138.46
5	3	9.20	2.95	6.24	44.89	93.82
6	4	54.69	16.97	37.86	269.18	135.59
23	5	40.38	20.41	30.19	215.23	102.14
16	6	60.36	22.89	43.12	302.64	149.74
12	7	51.97	27.06	40.41	292.52	133.69
15	8	68.27	25.64	48.38	347.09	109.55
20	9	82.17	29.73	55.93	410.47	134.84
2	10	41.01	24.68	30.75	235.14	104.44
9	11	16.63	5.23	11.63	81.34	92.53
3	12	14.89	17.52	10.96	87.50	106.82
18	13	15.47	6.20	10.71	77.39	97.54
26	14	33.56	19.32	23.39	179.36	121.45
1	15	15.61	21.24	12.62	100.78	83.22
7	16	12.87	6.51	9.42	68.05	105.75
8	17	69.18	33.47	51.40	364.29	135.95
11	18	21.45	11.24	15.77	114.82	110.09
27	19	35.61	20.50	24.59	185.12	115.79
21	20	30.47	10.52	21.17	151.95	90.95
14	21	10.70	4.09	7.38	53.14	109.29
17	22	4.98	1.82	3.47	24.52	74.05
19	23	32.40	12.00	23.07	161.80	117.45
13	24	11.21	4.62	7.91	56.17	79.65
10	25	40.60	14.70	28.34	204.05	118.44
4	26	44.49	20.94	31.15	236.20	137.35
22	27	30.23	10.95	21.42	150.39	129.04

ANOVA results in Table 4 for distortion show significant effect of feed, depth of cut and width of cut on distortion. Speed does not have significant effect on distortion. Strong interaction effects were observed between cutting parameters for distortion. The most significant interaction effects were found between feed - speed; feed - depth of cut; feed - width of cut; width of cut - depth of cut. It can be observed from the squared terms of

Table 4 that there is significant evidence of a quadratic effect. Figure 5 shows the direct effects of machining parameters on distortion. It is observed that increase in feed rate, depth of cut and width of cut increases distortion. This can be attributed to increase in forces in Z direction, torque and temperature. Interaction plots in Figure 6 for distortion show that, at higher levels of feed and width of cut there is pronounced increase in distortion with increase in depth of cut. ANOVA results from Table 4 for twist show that cutting speed, feed, depth of cut and width of cut all have significant effect on twist. Strong interaction effects exist between feed-depth of cut, feed-width of cut, depth of cut – width of cut and speed - depth of cut. Also, the squared terms of Table 4 show significant quadratic effect. It can be seen from direct effects plots for twist in Figure 7 that increase in feed, depth of cut and width of cut increases twist. It can also be seen that there is steep increase in twist at higher levels of depth of cut. It can be seen from interaction plots for twist in Figure 8 that at higher levels of feed, increase in twist is more pronounced with increase in cut.

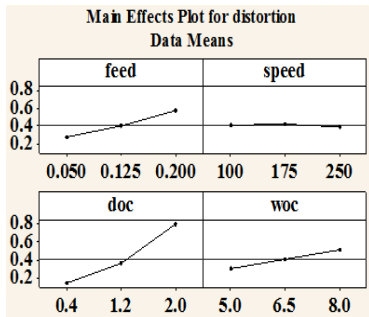


Figure 5: Direct plots for distortion.

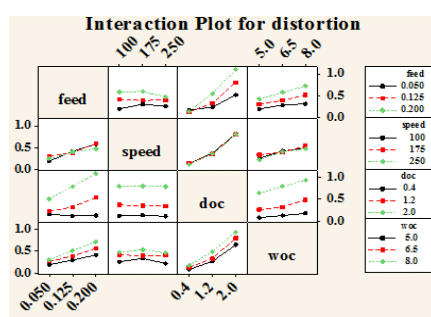


Figure 6: Interaction plots of distortion.

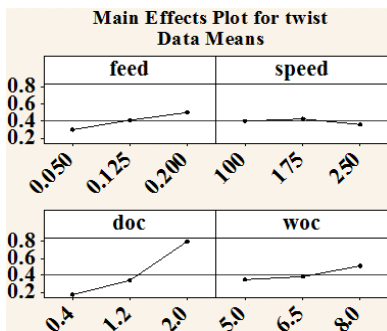


Figure 7: Direct plots for twist.

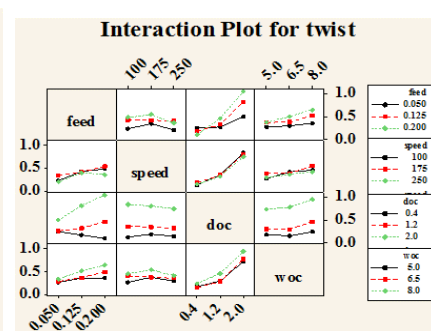


Figure 8: Interaction plots of twist.

Analysis of simulation results

Analysis of variance (ANOVA) was performed for simulated average cutting forces in X, Y, Z, torque and temperature and is shown in Table 5 and Table 6 respectively. Figure 12 show simulation graph of forces in Z direction. Direct effect plots are shown in Figure 9 and interaction effect plots are shown in Figure 10. It can be observed from ANOVA as shown in Table 5 and direct effect plots shown in Figure 9 that there is slight increase in forces in X and Y direction with increase in feed, depth of cut and width of cut, but have statistically insignificant effect on forces in X and Y direction. There is significant interaction effect of feed - depth of cut on cutting forces in X and Y directions. Interaction plots in Figure 10 indicate more increase in X and Y direction forces at higher feeds and depth of cuts. Test of ANOVA as shown in Table 5 and Table 6 for cutting forces in Z direction and torque show significant effect of feed, depth of cut and width of cut on cutting forces in Z direction and torque. Direct effect plots in Figure 9 indicate increase in forces in Z direction and torque with increase in feed, depth of cut and width of cut. There are significant interaction effects of feed - depth of cut, feed - width of cut and depth of cut - width of cut on forces in Z direction and torque. It can also be seen in Figure 10 of interaction plots for Z direction forces and torque that at higher feed, depth of cut and width of cut there is pronounced increase in forces in Z direction and torque. ANOVA shown in Table 6 indicate significant effect of all cutting parameters i.e., feed, speed, depth of cut and width of cut on temperature generated during cutting at cutting zone. Direct effect plots of temperature in Figure 9 show increase in cutting temperature with increase in feed, speed, depth of cut and width of cut. It can also be seen from ANOVA Table 6 and interaction plot for temperature from Figure 10 that there are no interaction effects of cutting parameters on cutting temperature.

Optimization

Two responses i.e., distortion and twist were considered for optimization simultaneously. The best combination levels should produce minimum distortion and twist. Maximum total desirability factor settings are considered for optimal conditions. Table 7 shows the inputs for multi response optimization. The Composite desirability function analysis for targeted responses for minimum distortion and twist was done in Minitab 16, using Equation (1) and Equation (2). Optimum parameters for minimum distortion with composite desirability 0.925 is given in Table 8. Figure 11 shows the desirability analysis graph with values in square brackets as optimum values. Response optimization shows optimal parameter combination range with composite desirability, with 0 target response of distortion and twist as, feed 0.18 to 0.2 mm/tooth, speed 180 to 210 m/min., depth of cut 0.4 mm and width of cut 5.6 mm. Table 9 shows, suggested optimum values of parameters, with values less than 0.09 mm for which validation experiments were carried.

Confirmation experiments

With the optimum input parameter values shown in Table 9, confirmation experiments were carried out for validation. Table 10 shows the predicted and actual values achieved from the validation experiments. It can be seen that there is an error of less than 10 % for predicted and actual values of distortion and twist with target value of 0.09 mm.

Table 4: Analysis of variance for distortion and twist.

Source	DF	Distortion			Twist		
		Sum of squares	Mean of squares	p	Sum of squares	Mean of squares	P
Regression	14	1.97017	0.14073	0	1.71995	0.12285	0
Linear	4	1.74107	0.43527	0	1.38135	0.34534	0
A-Feed	1	0.27	0.27	0	0.12201	0.12201	0
B-Speed	1	0.0012	0.0012	0.097	0.00441	0.00441	0.018
C-Depth of cut	1	1.33333	1.33333	0	1.17813	1.17813	0
D-Width of cut	1	0.13653	0.13653	0	0.0768	0.0768	0
Square	4	0.1095	0.02737	0	0.1942	0.04855	0
A*A	1	0.02253	0.02253	0	0.0106	0.0106	0.001
B*B	1	0.0048	0.0048	0.004	0.00156	0.00156	0.13
C*C	1	0.10453	0.10453	0	0.16961	0.16961	0
D*D	1	0.01333	0.01333	0	0.04646	0.04646	0
Interaction	6	0.1196	0.01993	0	0.1444	0.02407	0
A*B	1	0.00723	0.00723	0.001	0.00203	0.00203	0.088
A*C	1	0.09302	0.09302	0	0.1225	0.1225	0
A*D	1	0.0081	0.0081	0.001	0.01	0.01	0.001
B*C	1	0	0	1	0.00303	0.00303	0.043
B*D	1	0.00023	0.00023	0.45	0.00122	0.00122	0.175
C*D	1	0.01103	0.01103	0	0.00562	0.00562	0.009
Residual	Error	0.00443	0.00443		0.00706	0.00706	
Lack-of-Fit	10	0.00397	0.0004	0.427	0.00646	0.00065	0.359
Pure	Error	0.00047	0.00047		0.0006	0.0006	
Total	26						

Table 5: ANOVA for average cutting forces in X Y and Z direction.

Source	DF	Forces in X			Forces in Y			Forces in Z		
		Sum of squares	Mean of squares	P	Sum of squares	Mean of squares	P	Sum of squares	Mean of squares	P
Regression	14	10907.8	779.127	0	1880.54	134.325	0	5541.88	395.85	0
Linear	4	10.4	2.603	0.821	45.22	11.304	0.473	5254.39	1313.6	0
A-Feed	1	2.3	2.338	0.571	0.46	0.465	0.847	1195.52	1195.52	0
B-Speed	1	1.9	1.885	0.611	0.08	0.082	0.936	3.56	3.56	0.321
C-Depth of cut	1	1.9	1.922	0.607	3.68	3.682	0.59	3838.95	3838.95	00
D-Width of cut	1	1.4	1.362	0.665	34.61	34.608	0.115	216.37	216.37	0
Square	4	175.4	43.85	0.006	156.38	39.096	0.05	74.16	18.54	0.009
A*A	1	103.1	103.087	0.002	13.59	13.591	0.308	37.79	37.79	0.006
B*B	1	5.6	5.584	0.386	0.09	0.094	0.931	0.03	0.03	0.923
C*C	1	17.9	17.932	0.133	121.86	121.86	0.008	6.39	6.39	0.191
D*D	1	0.3	0.3	0.838	50.29	50.288	0.063	5.57	5.57	0.22

Effect of cutting parameters on machining induced distortion in thin wall thin floor parts

Interaction	6	443.8	73.972	0	97.73	16.289	0.307	213.33	35.56	0
A*B	1	4.4	4.421	0.439	0	0	0.997	1.05	1.05	0.584
A*C	1	385.6	385.558	0	44.58	44.575	0.078	164.1	164.1	0
A*D	1	10.7	10.703	0.237	10.06	10.06	0.378	15.73	15.73	0.05
B*C	1	13.7	13.688	0.184	1.24	1.236	0.754	5.61	5.61	0.219
B*D	1	0.2	0.211	0.864	0.02	0.018	0.97	0	0	1
C*D	1	29.3	29.252	0.062	41.84	41.842	0.087	26.85	26.85	0.015
Residual	Error	82.8	82.8	-	144.15	144.15		39.94	39.94	
Lack-of-Fit	10	71	7.104	0.534	142.59	14.259	0.053	34.45	3.45	0.522
Pure	Error	11.7	11.7		1.56	1.56		5.48	5.48	
Total	26									

Table 6: Analysis of variance for average temperature and torque.

Source	DF	Torque			Temperature		
		Sum of squares	Mean of squares	P	Sum of squares	Mean of squares	P
Regression	14	286780	20484	0	10141.6	724.4	0
Linear	4	272447	68112	0	9546.7	2386.68	0
A-Feed	1	65269	65269	0	1683.6	1683.61	0
B-Speed	1	285	285	0.143	3359.1	3359.13	0
C-Depth of cut	1	195413	195413	0	4144.1	4144.06	0
D-Width of cut	1	11480	11480	0	359.9	359.93	0
Square	4	2213	553	0.015	500.3	125.08	0.002
A*A	1	1777	1777	0.002	331.4	331.41	0
B*B	1	28	28	0.632	89.9	89.93	0.029
C*C	1	4	4	0.853	76.5	76.47	0.041
D*D	1	0	0	0.955	13.9	13.94	0.347
Interaction	6	12120	2020	0	94.5	15.75	0.426
A*B	1	51	51	0.518	21.7	21.74	0.245
A*C	1	9585	9585	0	9.3	9.31	0.44
A*D	1	756	756	0.025	1.3	1.34	0.767
B*C	1	429	429	0.078	27.8	27.84	0.192
B*D	1	5	5	0.843	0.8	0.79	0.82
C*D	1	1294	1294	0.006	33.5	33.47	0.155
Residual	Error	1388	1388		174.8	174.8	
Lack-of-Fit	10	1204	120	0.508	156.9	15.69	0.418
Pure	Error	184	184		17.9	17.9	
Total	26						

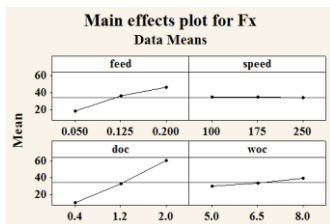
Discussion of results

Effects of machining parameters i.e., cutting speed, feed, depth of cut and width of cut were studied on machining induced distortion and twist. Machining parameters have significant effect on distortion and twist. Depth of cut, width of cut followed by feed were found to have significant effect on distortion. Increase in feed, depth of cut and width of cut lead to increase in distortion as shown from Figure 5. At higher levels of feed, increase in depth of cut and width of cut has pronounced effect on increase in distortion as shown from Figure 6. This can be attributed to significant increase in forces in Z

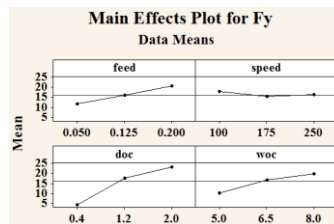
direction and increase in temperature gradient with increase in depth of cut and width of cut. Similarly, increase in feed, depth of cut and width of cut lead to increased twist in the component. More pronounced effect was found for depth of cut as shown in Figure 7. This increase in cutting forces and temperature with increase in feed, depth of cut and width of cut due to increase in length and width of engagement of flutes, leads to increased residual stress generation in subsurface and surface of the part due to coupled thermal and mechanical loads [3, 38]. Release of the part from the fixture cause imbalance in the induced stresses and distort the part during re-equilibration. So, optimum selection of cutting parameters will lead to reduced cutting forces and temperature in cutting zone and will lead to reduced distortion.

Table 7: Input parameters for multi response optimization.

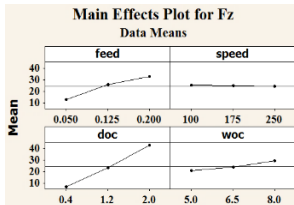
Sl. No.	Response	Goal	Target value	Upper value	Weight	Importance
1	Distortion	minimize	0	1.1	1	1
2	Twist	minimize	0	1.05	1	1



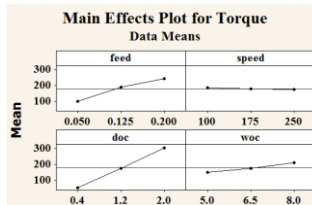
a) Main effects plot for force in X



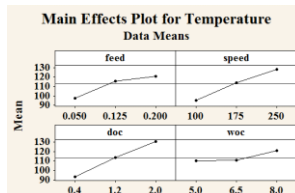
b) Main effects plot for force in Y



c) Main effects plot for force in Z



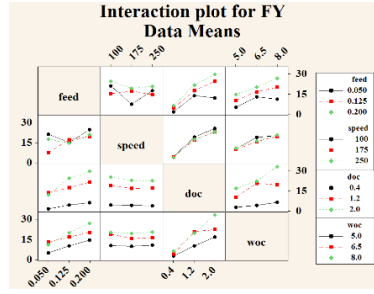
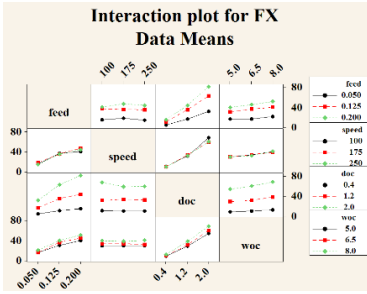
d) Main effects plot for Torque



e) Main effects plot for Temperature

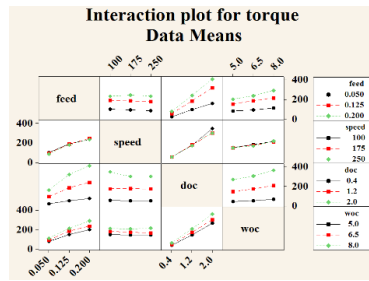
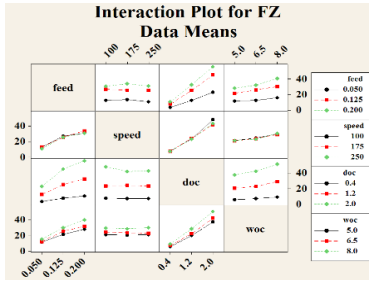
Figure 9: Direct effects plots for forces, torque and temperature.

Effect of cutting parameters on machining induced distortion in thin wall thin floor parts



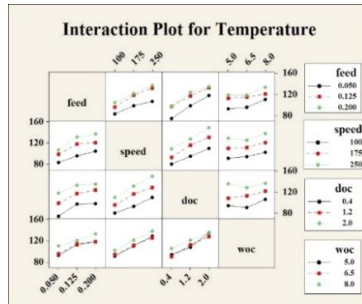
a) Interaction plots for Force in X

b) Interaction plots for Force in Y



c) Interaction plots for Force in Z

d) Interaction plots for Torque



e) Interaction plots for Temperature

Figure 10: Intraction effects plots for forces, torque and temperature

Table 8: Values for minimum distortion and twist.

Output response	Desirability	Response value	Optimum parameter					Composite desirability
			Feed (mm/tooth)	Speed (m/min.)	Depth of cut (mm)	Width of cut (mm)		
Distortion	0.932	0.074	0.18	210	0.4	5.6	0.925	
Twist	0.918	0.0855						

Table 9: Optimum parameters for target response.

Feed	Speed	DC	WC	Desirability for distortion	Desirability for twist	Composite desirability	Predicted distortion	Predicted twist
0.18	210	0.4	5.6	0.93	0.91	0.925	0.074	0.0855
0.19	215	0.4	5.6	0.92	0.92	0.925	0.079	0.080
0.2	220	0.4	5.6	0.92	0.92	0.923	0.087	0.077

Table 10: Comparison of actual and predicted values of validations.

Feed	Speed	DC	WC	Predicted distortion	Distortion Actual value	% error	Pred. twist	Twist Actual value	% error
0.18	210	0.4	5.6	0.074	0.068	-8.82	0.0855	0.082	-4.26
0.19	215	0.4	5.6	0.079	0.072	-9.72	0.080	0.09	7.98
0.2	220	0.4	5.6	0.087	0.088	1.13	0.077	0.085	9.41

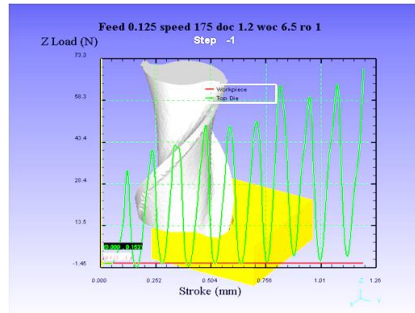
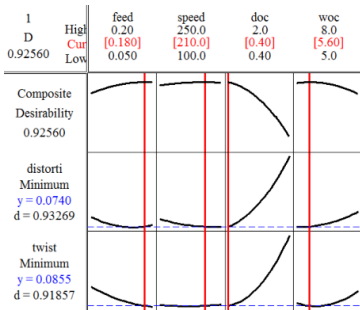


Figure 11: Optimization graph

Figure 12: Simulation graph for force in Z

Conclusions

Effect of cutting parameters on machining induced distortion of thin-wall thin-floor components was investigated by carrying out machining experiments on aluminium alloy 2014 using Box-Behnken Design (BBD).

The following are the conclusions:

- There is significant effect of feed, depth of cut and width of cut on distortion and twist during machining of thin-wall thin-floor components and cutting speed does not have significant effect on distortion in response space.
- Increase in temperature gradient and cutting forces with increase in width of cut and depth of cut lead to increase in distortion and twist.

- There is a prominent increase in distortion and twist with increase in feed rate at higher depth of cut and width of cut. So, use of lower depth of cut and width of cut at moderate feed rates leads to less distortion.
- The optimal combination of cutting parameters with target values of distortion and twist less than 0.09 mm is feed 0.18 to 0.2 mm/tooth, speed 180 to 210 m/min., width of cut 5.6 mm and depth of cut 0.4 mm.

Acknowledgement

The authors are very much thankful to the Head of Department, Osmania University for the constant encouragement and support in providing facilities for smooth conduct of experiments. The authors are also thankful to all those who were directly or indirectly helpful in conduct of experiments.

References

- [1] Denkena, B., and L. de León. "Machining induced residual stress in wrought aluminium parts." In *Proceedings of 2nd International Conference on Distortion Engineering, Germany*, pp. 107-114 (2008).
- [2] Chantzis, D., S. Van-der-Veen, J. Zettler, and W. M. Sim. "An industrial workflow to minimise part distortion for machining of large monolithic components in aerospace industry." *Procedia CIRP* 8: 281-286 (2013).
- [3] Li, Jian-guang, and Shu-qi Wang. "Distortion caused by residual stresses in machining aeronautical aluminum alloy parts: recent advances." *The International Journal of Advanced Manufacturing Technology* 89, no. 1-4: 997-1012 (2016).
- [4] Sim, Wei-Ming. "Challenges of residual stress and part distortion in the civil airframe industry." *International Journal of Microstructure and Materials Properties* 5, no. 4: 446-455 (2010).
- [5] Chatelain, Jean-François, Jean-François Lalonde, and Antoine S. Tahan. "Effect of residual stresses embedded within workpieces on the distortion of parts after machining." *Int J Mech* 6, no. 1: 43-51 (2012).
- [6] D'Alvise, L., D. Chantzis, B. Schoinochoritis, and K. Salonitis. "Modelling of part distortion due to residual stresses relaxation: an aeronautical case study." *Procedia CIRP* 31: 447-452 (2015).
- [7] Sim, Wei-Ming. *Residual Stress Engineering in Manufacture of Aerospace Structural Parts*. Filton, UK: Airbus SAS (2009).
- [8] K. Ma, R. Goetz, and S. K. Srivasta, "Modeling of residual stress and machining distortion in aerospace components (preprint)," *Enterprise Soc.*, vol. 9, no. 3, pp. 513-516, 2010.
- [9] Hornbach, D., and P. Prevéy. "Development of machining procedures to minimize distortion during manufacture." In *ASM Proceedings of 17th*

- Heat Treating Society Conference and Exposition: Heat Treating*, pp. 13-18. (1998).
- [10] Cui, Hengbo, Jong-Yun Jung, and Dug-Hee Moon. "The selection of machining parameters to minimize deformation caused by heat." In *Proceedings of the Fall Conference of Society of Korea Industrial and Systems Engineering*. (2005).
- [11] DONG, Hui-yue, and Ying-lin KE. "Study on machining deformation of aircraft monolithic component by FEM and experiment." *Chinese Journal of Aeronautics* 19, no. 3: 247-254 (2006).
- [12] Yeung, Millan K., and Peter Orban. "Spiral-layer machining for making thin-wall structures." In *Materials science forum*, vol. 505, pp. 877-882. Trans Tech Publications, (2006).
- [13] Jung, Jong-Yun, Heng-Bo Cui, Dug-Hee Moon, and Choon-Man Lee. "Parameter Selection for the Milling of Thin Wall." *Journal of the Society of Korea Industrial and Systems Engineering* 30 (2007).
- [14] Wei, Yu, and X. W. Wang. "Computer simulation and experimental study of machining deflection due to original residual stress of aerospace thin-walled parts." *The international journal of advanced manufacturing technology* 33, no.: 260-2653 (2007).
- [15] Younger, Mandy S., and Kenneth Hall Eckelmeyer. "Overcoming residual stresses and machining distortion in the production of aluminum alloy satellite boxes." No. SAND2007-6811. Sandia National Laboratories (2007).
- [16] Pierard, O., J. Barboza, M. DufLOT, L. D'Alvise, and A. Perez-Duarte. "Distortions prediction during multi-pass machining simulations by using the level-set method." *International journal of material forming* 1, no. 1: 563-565 (2008).
- [17] Guo, H., D. W. Zuo, H. B. Wu, F. Xu, and G. Q. Tong. "Prediction on milling distortion for aero-multi-frame parts." *Materials Science and Engineering: A* 499, no. 1: 230-233 (2009).
- [18] Bi, Yun-bo, Qun-lin Cheng, Hui-yue Dong, and Ying-lin Ke. "Machining distortion prediction of aerospace monolithic components." *Journal of Zhejiang University-SCIENCE A* 10, no. 5: 661-668 (2009).
- [19] Zhou, Zebin, Jianguo Yang, and Beizhi Li. "Machining simulation and deformation prediction in the processing for thin-walled parts." In *Systems and Control in Aeronautics and Astronautics (ISSCAA), 2010 3rd International Symposium on*, pp. 256-261. IEEE (2010).
- [20] Tang, Zhi Tao, Zhan Qiang Liu, and Li Qiang Xu. "Effect of Process Routing on Machining Deformation for Multi-Frame Double Sided Monolithic Components." In *Advanced Materials Research*, vol. 97, pp. 2894-2897. Trans Tech Publications (2010).
- [21] Yang, Yong, and Yu-Ling Wang. "Analysis and control of machining distortion for aircraft monolithic component aided by computer."

- In *Information and Computing (ICIC), 2010 Third International Conference on*, vol. 3, pp. 280-283. IEEE (2010).
- [22] Chatelain, Jean-François, J. F. Lalonde, and A. S. Tahan. "A comparison of the distortion of machined parts resulting from residual stresses within workpieces." In *Proceedings of the 4th International Conference on Manufacturing Engineering, Quality and Production Systems (MEQAPS'11)*, pp. 79-84 (2011).
- [23] Zhongyi, Mei, Wang Yunqiao, and Amir Saleem. "Distortion analysis of arc shaped workpiece in NC machining." In *Proceedings of the World Congress on Engineering*, vol. 3. (2011).
- [24] Keleshian, N., R. Kyser, J. Rodriguez, C. Cueva, V. Vega, E. W. Lee, J. Ogren, and Omar S. Es-Said. "On the distortion and warpage of 7249 aluminum alloy after quenching and machining." *Journal of materials engineering and performance* 20, no. 7: 1230-1234 (2011).
- [25] Ye, Hai Chao, Guo Hua Qin, Cong Kang Wang, and Dong Lu. "A simulation study on the end milling operation with multiple process steps of aeronautical frame monolithic components." In *Applied Mechanics and Materials*, vol. 66, pp. 569-572. Trans Tech Publications (2011).
- [26] Wang, Yun Qiao, Zhong Yi Mei, and Yu Qing Fan. "Research on Machining Distortion due to Residual Stresses of Large Monolithic Beam." In *Advanced Materials Research*, vol. 433, pp. 530-537. Trans Tech Publications (2012).
- [27] Guo, Hun. "The Influence of Residual Stress on the Machining Deformation." In *Advanced Materials Research*, vol. 426, pp. 172-176. Trans Tech Publications (2012).
- [28] Jiang, Xiaohui, Beizhi Li, Jianguo Yang, and Xiao Zuo. "Effects of tool diameters on the residual stress and distortion induced by milling of thin-walled part." *International Journal of Advanced Manufacturing Technology* 68 (2013).
- [29] Schulze, V., P. Arrazola, F. Zanger, and J. Osterried. "Simulation of distortion due to machining of thin-walled components." *Procedia CIRP* 8: 45-50 (2013).
- [30] Yang, Y., M. Li, and K. R. Li. "Comparison and analysis of main effect elements of machining distortion for aluminum alloy and titanium alloy aircraft monolithic component." *The International Journal of Advanced Manufacturing Technology* 70, no. 9-12: 1803-1811 (2014).
- [31] Cao, Yan, Yu Bai, Yongqiang He, Jianhui Tian, and Yunlong Li. "NC Milling Deformation Forecasting of Aluminum Alloy Thin-Walled Workpiece Based on Orthogonal Cutting Experiments and CAD/CAM/FEA Integration Paper Title." *International Journal of Control and Automation* 7, no. 9: 67-80 (2014).
- [32] Song, Qinghua, Zhanqiang Liu, and Xing Ai. "Influence of Chatter on Machining Distortion for Thin-Walled Component Peripheral

- Milling." *Advances in Mechanical Engineering* 6: 329564 (2014).
- [33] Cerutti, Xavier, and Katia Mocellin. "Prediction of Post-Machining Distortion Due to Residual Stresses Using FEM and a Massive Removal Approach." In *Key Engineering Materials*, vol. 611, pp. 1159-1165. Trans Tech Publications (2014).
- [34] Haiyang, Yuan, Wu Yunxin, Gong Hai, and Wang Xiaoyan. "A milling deformation model for aluminum alloy frame-shaped workpieces caused by residual stress." *Mechanics* 21, no. 4: 313-322 (2015).
- [35] Jain, Anil Kumar, Kasala Narasaiah, and Shibu Gopinath. "Machining of Thin Walls and Thin Floor Aerospace Components Made of Aluminum Alloy with High Aspect Ratio." In *Materials Science Forum*, vol. 830, pp. 112-115. Trans Tech Publications (2015).
- [36] Sridhar, Garimella, and Ramesh Babu Poosa. "Volume of material removal on distortion in machining thin wall thin floor components." *Int J Mech Eng Applications* 3, no. 5: 86-93 (2015).
- [37] Sridhar, G., and P. Babu Ramesh. "Effect of a milling cutter diameter on distortion due to the machining of thin wall thin floor components." *Advances in Production Engineering & Management* 10, no. 3: 140 (2015).
- [38] Masoudi, Soroush, Saeid Amini, Ehsan Saeidi, and Hamdollah Eslami-Chalander. "Effect of machining-induced residual stress on the distortion of thin-walled parts." *The International Journal of Advanced Manufacturing Technology* 76, no. 1-4: 597-608 (2015).
- [39] Kaufman, J. Gilbert. *Introduction to aluminum alloys and tempers*. (ASM international, 2000).
- [40] Davis, Joseph R. *Metals handbook*. (ASM international, 1998).
- [41] Aslan, N., and Y. Cebeci. "Application of Box-Behnken design and response surface methodology for modeling of some Turkish coals." *Fuel* 86, no. 1: 90-97 (2007).
- [42] Myers, Raymond H., Douglas C. Montgomery, and Christine M. Anderson-Cook. *Response surface methodology: process and product optimization using designed experiments*. (John Wiley & Sons, 2016).
- [43] Yanda, Hendri, Jaharah A. Ghani, and Che Hassan Che Haron. "Effect of rake angle on stress, strain and temperature on the edge of carbide cutting tool in orthogonal cutting using FEM simulation." *Journal of Engineering and Technological Sciences* 42, no. 2: 179-194 (2010).
- [44] Gardner JD, Vijayaraghavan A, Dornfeld DA. Comparative study of finite element simulation software. In: Lab Manuf Autom <http://escholarship.org/uc/item/8cw4n2tf>. Accessed 28 January, 2013.
- [45] Candioti, Luciana Vera, María M. De Zan, María S. Cámara, and Héctor C. Goicoechea. "Experimental design and multiple response optimization. Using the desirability function in analytical methods development." *Talanta* 124: 123-138 (2014).